Directing the Deformation Paths of Soft Metamaterials with Prescribed Asymmetric Units

*Gaoxiang Wu, Yigil Cho, In-Suk Choi, Dengteng Ge, Ju Li, Heung Nam Han, Tom Lubensky, and Shu Yang**

Metamaterials are artificially engineered materials whose physical properties are functions of the structural parameters of the underlying periodic microstructures, including shape, geometry, size, orientation, and arrangement. Soft metamaterials with reconfigurable microstructures in response to external stimuli are thus of great interest for their switching behavior with potential applications, including miniaturized devices,[1–3] microactuation,[3–6] optical manipulation,[7,8] microfluidic devices,[9] and drug delivery.[10] However, deformation, if not controlled, could lead to failure that can interfere with the performance of devices.

Recently, we and others have explored buckling instabilities of soft membranes with periodic hole arrays, where the bending of the interpore ligaments triggers homogeneous and reversible pattern transformations.[11–26] The transformation occurs at a broad range of length scales ranging from submicron[14,16,19,20] to centimeter scale,[11,21,26] and offers a unique mechanism to induce significant change of the physical properties of the metamaterials, including photonic[27,28] and phononic[24] bandgaps, mechanical properties (e.g., negative Poisson's ratio),[17,21] and symmetry breaking[24,25] arising from simultaneous alterations of lattice symmetry, pore size and shape, and volume filling fraction. Meanwhile, there has been significant effort in theoretical understandings of mechanical behaviors of periodic structures with respect to geometry, including rectangular,[29–35] chiral honeycomb,[36–38] and triangular structures,[39–42] via rotation of the basic units.

Despite these advances, challenges remain. For example, mechanical instability accompanied with compression of the periodically porous structures often leads to sudden structural change, and thus change of mechanical properties, above the critical buckling threshold. The deformation path of a porous structure is often limited to the one with the lowest elastic energy increment (i.e., the buckling mode with the lowest eigenvalue), whereas those with higher eigenvalues are not readily accessible.[26] Further, unwanted structural defects (e.g., anti-phase boundaries) originated from inhomogeneity introduced during the fabrication or uneven external loading, are often produced during the deformation process. Therefore, controllability over the entire structure during deformation needs to be investigated, in particular, to direct the deformation paths and prevent mechanical instabilities and/or possible structural defects.

Here, we chose kagome lattices with triangular structure units as the model system to address the above issues. Among various two-dimensional (2D) lattices that undergo periodic collapse mechanisms, the kagome lattices (also referred as trihexagonal tiling) and related lattices offer many desirable transport and elastic properties, heat-dissipation characteristics, and large photonic bandgaps.[43–48] The twisted kagome and related lattices exhibit isotropic elasticity with a vanishing bulk modulus.[39] More importantly, kagome lattices of N lattice sites can have an order of $N^{1/2}$ "floppy" modes of lattice distortion under free boundary conditions, that is, they have $N^{1/2}$ modes of low-energy deformations of the structures via rotation of neighboring "rigid" structural units (here triangles) against each other without distorting the triangles. Correspondingly, kagome lattices could exhibit maximal negative Poisson's ratio −1.[49] Therefore, kagome lattices offer an ideal model to investigate how to control the deformation path upon expansion and contraction, and the production of large deformations in response to relatively small external perturbations – a highly attractive feature for applications of mechanical metamaterials.

Guided by finite-element (FE) modeling, we designed and fabricated periodic, porous membrane structures with asymmetric ligaments in kagome lattices prescribed with a pretwisting angle. These designs not only prevented buckling instabilities but also offered deterministic pattern transformations guided by the asymmetric interpore ligaments. We investigated the mechanical response and structural evolution of these soft metamaterials upon mechanical compression both numerically and experimentally. We found that structural reconfiguration behaviors were strongly affected by the asymmetric nature of

G. Wu, Dr. Y. Cho, Dr. D. Ge, Prof. S. Yang
Department of Materials Science and Engineering
University of Pennsylvania
3231 Walnut Street, Philadelphia, PA 19104, USA
E-mail: shuyang@seas.upenn.edu
Dr. Y. Cho, Dr. I.-S. Choi
High Temperature Energy Materials Research Center
Korea Institute of Science and Technology (KIST)
Seongbuk-gu Hwarang-ro 14–5, Seoul 136–791, South Korea
Prof. J. Li
Department of Nuclear Science and Engineering
and Department of Materials Science and Engineering
Massachusetts Institute of Technology
77 Massachusetts Ave, Cambridge, MA 02139, USA
Prof. H. N. Han
Department of Materials Science and Engineering
RIAM, Seoul National University
Gwanak-gu Gwanak-ro 1, Seoul 151–744, South Korea
Prof. T. Lubensky
Department of Physics and Astronomy
University of Pennsylvania
209 S. 33rd Street, Philadelphia, PA 19104, USA

DOI: 10.1002/adma.201500716

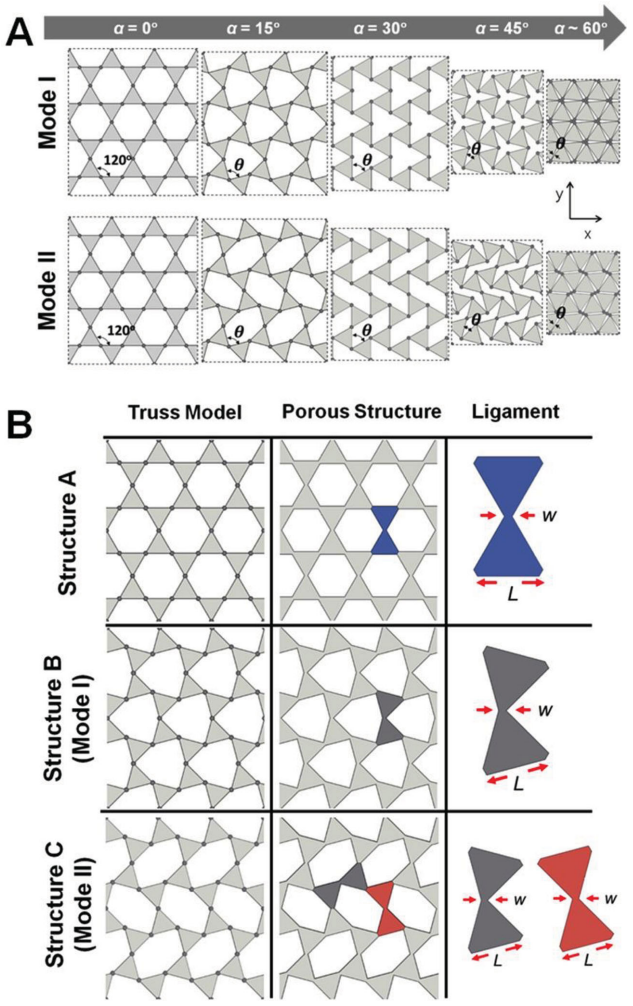

Figure 1. A) Schematic illustrations of the geometric model of a kagome lattice and the corresponding two collapsing modes. With increasing the twisting angle α from 0° to 60°, the lattice reaches full compaction. $\alpha = (120° - \theta)/2$. B) Schematics of three types of soft porous structures (structures A, B, and C) based on the periodic truss model of kagome lattices and the corresponding interpore ligaments with a pre-twisting angle $\alpha = 15°$.

the interpore ligaments, which in turn determined the attractive features of these soft metamaterials systems. Specifically, we could fine-tune the pathway of the structural change, the deformation mode, structural stiffness, and the achievable negative Poisson's ratio by prescribing the pore units with designated pre-twisting angles.

Prototypes of the kagome lattices were designed according to their geometric models, including rotating rigid units and hinge-jointed vertices. Two simple collapsing mechanisms are investigated (**Figure 1**A): Mode I, in which the triangular units rotates against every hinges and deformation is locally isotropic, and Mode II, the triangular units rotates against 2/3 of the hinges, producing a pattern of alternately tilted distorted hexagonal pores. Both collapsing mechanisms can be characterized by a single angle α specifying the direction of kagome triangles relative to the x-axis; $\alpha = (120° - \theta)/2$ where θ is the angle between two edges of interconnected triangular units (see Figure 1A). In both cases, as α increases from 0° (full extension) to 60° (full compaction), the lattice contracts in all directions by a factor of $\cos\alpha$, and the area of the lattice decreases by a factor of $\cos^2\alpha$, and thus the total area becomes 0.25 of the original area at full compaction ($\alpha = 60°$). This compaction is considerably higher than that of rotating square (theoretical value, 0.5) and, therefore, allows for wider design space in tunable soft metamaterials.

By replacing the hinges using thin polymer ligaments and the triangular units with bulk polymers, we create a series of kagome lattice based porous structures with and without pre-twisting (see Figure 1B). The beauty of this system is that the thin polymer ligaments have very low bending stiffness, M, compared to that of the triangular units, which is defined by $M = EC\kappa t^3$. Here, E is the elastic modulus, C is the geometric constant, κ is the curvature, and t is the width, which varies from w (at hinge) to L (at the triangular edge; see Figure 1B). Therefore, highly localized bending deformation is triggered at the ligaments, leading to pattern transformation via rotation of the ligaments. This implies that the designed characteristics of the ligaments will directly affect the overall mechanical behavior of the porous structures. Specifically, the relative bending stiffness of the ligaments can be tuned by the ratio L/w, and the pre-twisting angle α (see Figure 1A), which controls the nature of the ligaments: $\alpha = 0°$ for perfect symmetric ligaments, and $\alpha > 0°$ for asymmetric ligaments.

First, we focus on how the symmetry of the ligaments affects the overall mechanical response of the kagome lattices. We fixed the $L/w = 8$ ($L = 6$ mm, and $w = 0.75$ mm in both experiments and simulation), and created a porous structure from the non-twisted kagome lattice ($\alpha = 0°$, structure A), and two types of pre-twisted ($\alpha = 15°$) kagome lattices, including structure B with all ligaments pre-twisted, and structure C with only 2/3 of ligaments pre-twisted. The latter two represent the collapsing modes I and II, respectively (see Figure 1B). It is worth noting that this process is similar to that in the re-entrant foam structures, where the pre-applied compressive strain forces the foam ribs to bend inward. Here, through the introduction of the pre-twisted thin polymer ligaments, we essentially created two sets of 2D re-entrant structures from the kagome lattice with biaxial shrinkage of $2L(\cos\alpha - 1)/(2L + w)$ in both x and y directions. As shown in Figure 1B, at the same pre-twisting angle for collapsing modes I and II, both structures B and C have the same shaped asymmetric ligaments (shown as the dark gray blocks in Figure 1B), but their composition and arrangement in 2D are quite different. In experiments, a small pre-twisting angle (i.e., $\alpha = 15°$) was introduced in the original lattice such that the sample would experience minimal biaxial shrinkage (≈3.2%). Compared to structure A, the reduction of the porosity for structures B and C is only ≈1.8% (from 66.4% to 64.6% at $L/w = 8$). Such small difference in porosity generally does not lead to a significant change in the mechanical behavior of the overall structure.[17] However, it is sufficient to guide the bending direction of the ligaments, thus, inhibiting buckling in structures B and C. In structure A, at the buckling threshold each ligament has one independent choice of the bending direction because of the symmetric nature of the ligaments. In fact, in the previously reported deformation of periodic porous structures,[11,15,16,20,21,25] all i) require deformation

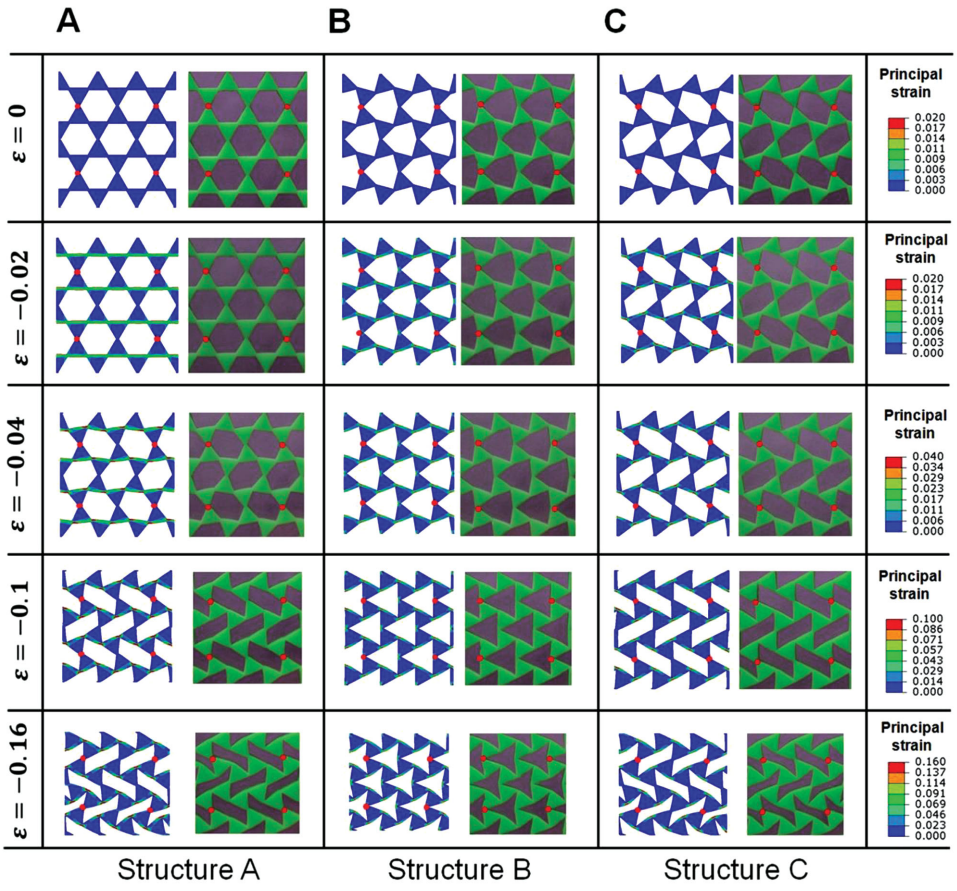

Figure 2. Numerical (left) and experimental (right) images of the deformation processes of three kagome-based lattices. A) Non-twisted, B) pre-twisted (Mode I), and C) pre-twisted (Mode II) structures. The twisted (collapsing) modes are defined in Figure 1. B and C have the same pre-twisting angle, $\alpha = 15°$, but different amounts of pre-twisted ligament (100% for B, and ≈67% for C). The principal strain shown in the legend represents the maximum principal strain.

above a buckling threshold to initiate bending, and consequently, ii) have a sudden change of structure above the buckling threshold, and iii) lack control of the bending direction of the individual ligament. For structure A, the non-deterministic bending led to incomplete compaction, especially under an inhomogeneous load (see Figure S1A and Movie S1, Supporting Information). In comparison, the pre-twisted kagome lattices (structures B and C) showed deterministic bending of ligaments even under an inhomogeneous load (Figure S1B,C and Movie S2 and S3, Supporting Information), and the porous membranes were completely closed.

To support our design, we built physical and numerical models of all three cellular solid structures consisting of 8 × 10 hexagonal or slightly deformed hexagonal voids (see Figure S2, Supporting Information). The soft porous structures were fabricated from silicone rubber through replica-molding of templates fabricated by 3D printing. On top and bottom of the samples, we intentionally left beam-like layers of silicone with 6 mm width (see Figure S2, Supporting Information), allowing for uniform compression. Uniaxial compression tests were performed by sandwiching the rubber sheet between two acrylic plates and a third acrylic plate was clamped to a load cell (see Movie S4–S6, Supporting Information). The overall deformation process and mechanical behaviors were simulated using the general purposed implicit FE code, ABAQUS/Standard, for interpretation of the mechanical deformation to the porous structures. In simulation, plane strain condition was used, and the behavior of the silicone rubber was captured using the Yeoh hyperelastic model.[38] The uniaxial compression tests were simulated by imposing vertical displacements at the top surface while keeping vertical movement on the bottom surface fixed. Along the horizontal direction, the structure could move freely.

Representative experimental images taken during the compression test were compared with simulation shown in **Figure 2** at different nominal strains ($\varepsilon_y = 0$, 0.02, 0.04, 0.1, and 0.16). Here, ε_y is defined by $(H_0 - H)/H_0$, where H_0 is the initial height of the structure and H is the height after compression. We focused on structural change at the central region of the samples, where the boundary effect was minimized. In all three cases, the experimental results showed excellent agreement with FE simulation, which captured mechanical response of the cellular solids to the nominal strain up to 16%.

During uniaxial compression, structure A with symmetric ligaments experienced buckling instability, that is an abrupt transition of the porous structure to an array of sheared

hexagons above the critical strain $\varepsilon_c \approx 0.033$ (see Movie S4, Supporting Information). The triggered buckling modes resembled the collapsing mode II in periodic truss model. After the buckling of the interpore ligaments, the deformation to the periodic porous structure was accommodated by further rotation of the triangular units and bending of the interpore ligaments. In comparison, an unevenly distributed strain level across the asymmetric ligaments in structures B and C were found even at a very small loading (e.g., $\varepsilon = -0.02$, see Figure 2B,C), thus, they bent immediately at the onset of the loading without experiencing any buckling instability. The microstructures evolved smoothly and strictly followed the collapsing modes prescribed by the asymmetric ligament structures (see Movie S5 and S6, Supporting Information). Specifically, we achieved a distinctive deformation path in structure B, where all of the interpore ligaments were bent simultaneously during the pattern transformation process. Such a deformation path is not achievable in normal compression of non-twisted kagome lattice because it has much higher eigenvalue than the one in structure A or C.[26] Our results suggest that it is possible to access a much richer range of deformation paths by introducing asymmetric ligaments to the cellular solid structures or mixing structures, for example, B and C with different portions and at different locations within the specimen as demonstrated in our earlier work.[35] As a result, different mechanical responses during compression will be obtained.

A more quantitative investigation was carried out by comparing experimental results with FE simulation following the evolution of the stress and Poisson's ratio vs. the applied nominal strain. For structure A, we observed a typical stress–strain behavior for the buckling induced pattern transformation process,[21] including a linear elastic regime, a stress plateau, and eventually a non-linear curve-up region (see **Figure 3**A). The departure from linearity is an indication of structural buckling and corresponds to the process of abrupt transition of the lattice geometry into sheared hexagons. The densification of the periodic porous structure at high compressive strain causes the curve-up in the stress–strain curve. For structures B and C, however, there was no clear transition from the linear elastic regime to a plateau regime; the stress–strain curves were smooth with a slope gradually decreased before reaching the densification (see Figure 3A). This observation is consistent with the smooth evolution of the microstructure during compression (see Movie S5 and S6, Supporting Information).

Noticeably, the three structures studied here showed very different flexibility. Structure A required the highest energy (proportional to the area under the stress–strain curve in Figure 3A) to reach a nominal strain of –0.1. This suggests that the presence of the pre-twisted ligament reduces the energy cost required for compacting the soft porous structures, a much desired property in designing foldable devices. Meanwhile, structure C was found to be more flexible than structure B. This difference in flexibility again is the direct result of different deformation paths of microstructures: deformation of structure B was accommodated by bending of every ligament, while only 2/3 of the ligaments in structure C were bent (see Figure 2). It was also found that the ratio between the integration of measured stress over strain from $\varepsilon = 0$ to –0.1 for structures B and C was also ≈3/2. Therefore, on average the

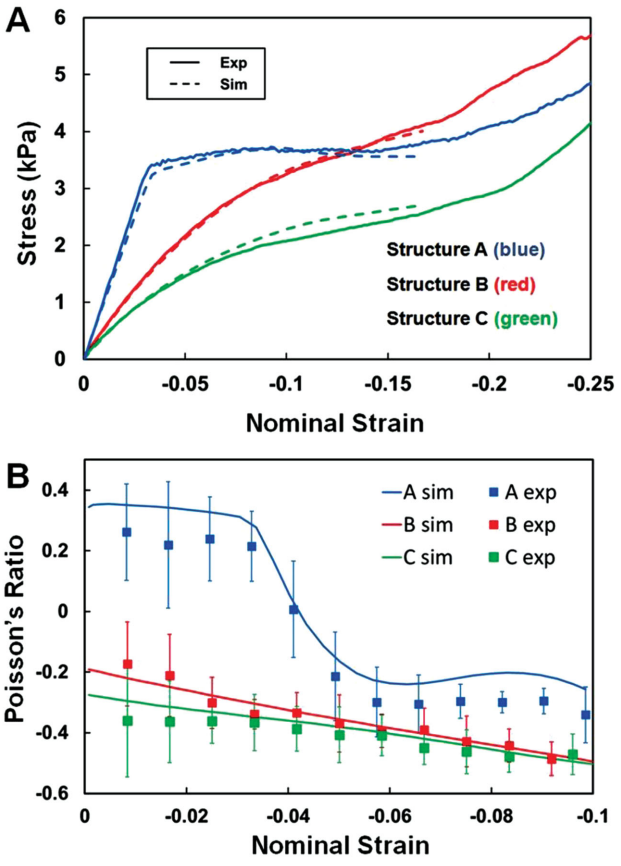

Figure 3. A) The stress–strain relationship of structures A, B, and C under uniaxial compression from both experiments and FE simulations. B) Macroscopic Poisson's ratio ν as a function of the nominal strain.

energy consumed in bending each ligament in structure B and C are approximately the same. This observation implies that the mechanical responses of the soft porous structures are not only related to the bending of the interpore ligaments, but also their arrangement.

It is well known that rotating rectangular or triangular units possess negative Poisson's ratio (or so-called auxetic behavior).[49] Figure 3B shows the average Poisson's ratio (ν) with respect to the applied nominal strain. ν is calculated from the ratio of the nominal strains in the horizontal edge to that in the vertical edge in the rectangular regions surrounded by four red dots (see Figure 2 and Figure S4, Supporting Information). It is clear that the introduction of the asymmetric ligaments to the cellular solid greatly affects the evolution of the Poisson's ratio during deformation. Structure A initially had a positive ν. Similar to the report in the literature on square arrays of circular pores,[17] the dramatic pattern transformation induced by the buckling of the interpore ligaments led to a monotonic decrease of ν as function of nominal strain and eventually became negative. Structures B and C were, however, strikingly different from A. They had negative Poisson's ratio from the start (ca. –0.2 for structure B, and ca. –0.3 for structure C), which underwent mild decays and leveled at values ca. –0.5 to –0.6 at a higher nominal strain. As a result, the negative Poisson's ratios achieved by structures B and C (with asymmetric

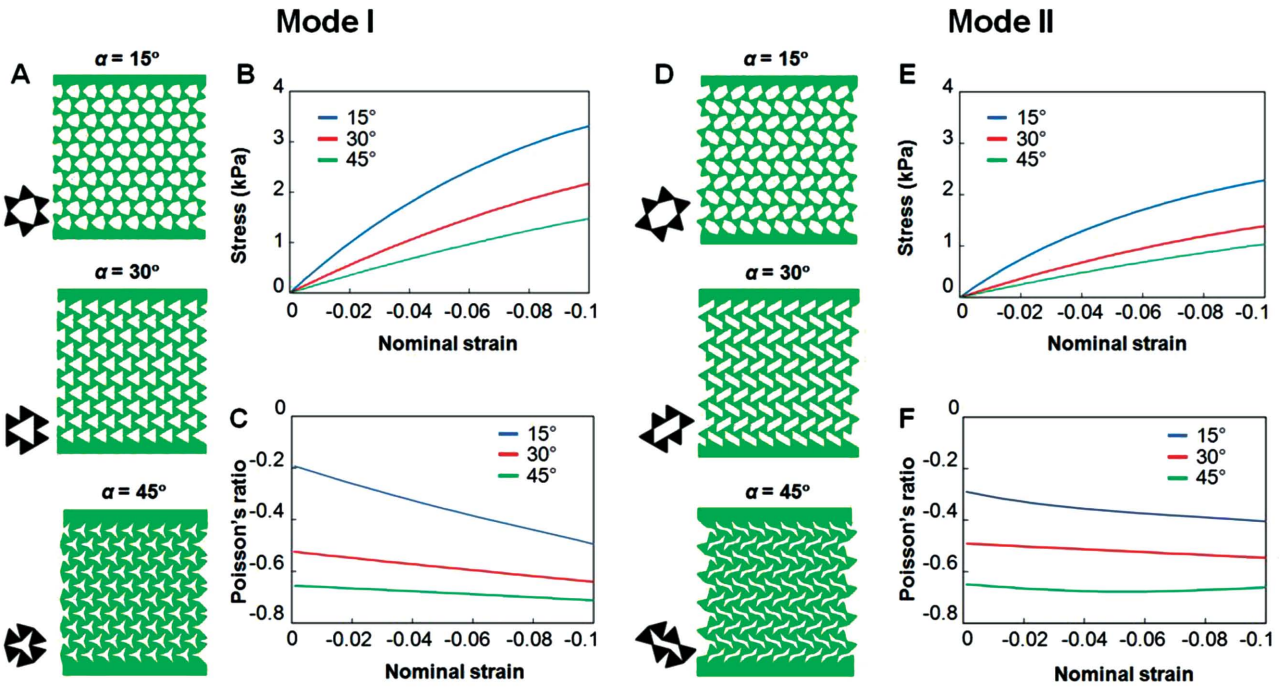

Figure 4. FE simulation of pre-twisted kagome lattices with different pre-twisting angles under uniaxial compression. A–C) Mode I. D–F) Mode II. A,D) The original non-deformed structures for modeling. B,E) Stress–strain relationship. C,F) The corresponding evolution of the Poisson's ratio.

ligaments) are considered as ready-to-use properties, This is distinctly different from structure A and other 2D porous structures reported in the literature,[17,21] where a significant pre-strain is often required (normally ≈5% to 10%) to achieve the negative Poisson's ratio.

We note that Grima and Evans have theoretically investigated mechanical behaviors of kagome lattices extensively,[40] providing a full description of the mechanical properties including Poisson's ratio and elastic moduli. The study, however, is derived from an idealized kagome structure where triangles are rigid and zero-width hinges have finite bending stiffness, resulting in Poisson's ratio of −1 regardless of the pre-twisting angle. This is different from our experimental and FE simulation results. We believe the discrepancy is originated from the non-ideal nature of the experimental system, where the triangle units are made of deformable silicone rubber and the hinges between them have a finite width. For structure A, the bending deformation of the ligaments and rotation of the triangles that mimic the collapsing path of kagome lattice are not triggered until reaching the buckling threshold of the entire structure. Therefore, the Poisson's ratio of structure A is positive at the beginning of the deformation, and thus exhibits the largest deviation from the ideal collapsing mechanisms.

To better exploit the utility of the pre-twisting angle, we performed simulation on the soft porous structures based on the collapsing modes I and II with different pre-twisting angles (15°, 30°, and 45°, see **Figure 4**A,D). As shown in Figure 4B,C,E,F, the mechanical response of the soft metamaterials, including flexibility and auxetic behavior, can be dynamically tuned simply by varying the pre-twisting angle. A large negative and stable value of Poisson's ratio is achieved from structures with a pre-twisting angle of 45°. These results are in sharp contrast to the theoretical study of ideal kagome lattices reported in the literature,[40] where the Poisson's ratio is kept constant, −1, irrespective of the twisting angle. By combining structures of different types of pre-twisted ligaments in various arrangements, we can fine-tune the range of negative Poisson's ratio and thus flexibility of the entire film and/or at local positions.

In summary, we studied the collapsing modes of pre-twisted kagome lattices with prescribed asymmetric ligaments in different arrangements. We successfully avoided the buckling instability, allowing for smooth and homogenous structural reconfiguration in a deterministic fashion. The mechanical responses of the designed metamaterials, including stress–strain behaviors and the resulting negative Poisson's ratios, are strongly affected by the symmetry of the ligaments and their arrangement. Here, we suggest a new and important design concept in soft metamaterials, that is, the introduction of asymmetric ligaments to the periodic porous structures. It will allow for exquisite control of the compaction path of the porous structures, thus reaching much richer range of transformed patterns and their corresponding physical properties. The knowledge presented here will also provide critical insights to design foldable or deployable devices by precise control of the materials stiffness and mechanical response in 2D and 3D sheets.

Supporting Information

Supporting Information is available from the Wiley Online Library or from the author.

Acknowledgements

G.W. and Y.C. contributed equally to this work. The research is funded by National Science Foundation (NSF), #DMR-1410253, and EFRI/ODISSEI grant, #EFRI-1331583. The Laboratory for Research on the Structure of Matter (LRSM) and Prof. Karen Winey's group at University of Pennsylvania are acknowledged for the access to an Instron machine. Prof. Pei-Chun Lin and Fu-Long Chang (National Taiwan University) are acknowledged for kindly fabricating the gadget to compress the porous structures. H.N.H. was supported by the Basic Science Research Program through the National Research Foundation of Korea (NRF) funded by the Ministry of Science, ICT and Future Planning (NRF-2013R1A2A2A01008806). Y.C. and I.-S.C. are supported by the Korea Institute of Science and Technology Global Research Program (Grant 2Z04050).
Note: The acknowledgements were updated on May 4, 2015, after initial publication online.

Received: February 10, 2015
Published online: March 23, 2015

[1] X. He, M. Aizenberg, O. Kuksenok, L. D. Zarzar, A. Shastri, A. C. Balazs, J. Aizenberg, *Nature* **2012**, *487*, 214.
[2] A. Sidorenko, T. Krupenkin, A. Taylor, P. Fratzl, J. Aizenberg, *Science* **2007**, *315*, 487.
[3] C. L. van Oosten, C. W. M. Bastiaansen, D. J. Broer, *Nat. Mater.* **2009**, *8*, 677.
[4] P. J. Glazer, J. Leuven, H. An, S. G. Lemay, E. Mendes, *Adv. Funct. Mater.* **2013**, *23*, 2964.
[5] J. le Digabel, N. Biais, J. Fresnais, J.-F. Berret, P. Hersen, B. Ladoux, *Lab Chip* **2011**, *11*, 2630.
[6] Z. L. Wu, M. Moshe, J. Greener, H. Therien-Aubin, Z. Nie, E. Sharon, E. Kumacheva, *Nat. Commun.* **2013**, *4*, 1586.
[7] L. Dong, A. K. Agarwal, D. J. Beebe, H. Jiang, *Nature* **2006**, *442*, 551.
[8] N. Shimamoto, Y. Tanaka, H. Mitomo, R. Kawamura, K. Ijiro, K. Sasaki, Y. Osada, *Adv. Mater.* **2012**, *24*, 5243.
[9] D. J. Beebe, J. S. Moore, J. M. Bauer, Q. Yu, R. H. Liu, C. Devadoss, B.-H. Jo, *Nature* **2000**, *404*, 588.
[10] J. D. Ehrick, S. K. Deo, T. W. Browning, L. G. Bachas, M. J. Madou, S. Daunert, *Nat. Mater.* **2005**, *4*, 298.
[11] T. Mullin, S. Deschanel, K. Bertoldi, M. C. Boyce, *Phys. Rev. Lett.* **2007**, *99*, 084301.
[12] K. Bertoldi, M. C. Boyce, S. Deschanel, S. M. Prange, T. Mullin, *J. Mech. Phys. Solids* **2008**, *56*, 2642.
[13] Y. Zhang, E. A. Matsumoto, A. Peter, P.-C. Lin, R. D. Kamien, S. Yang, *Nano Lett.* **2008**, *8*, 1192.
[14] S. Singamaneni, K. Bertoldi, S. Chang, J.-H. Jang, E. L. Thomas, M. C. Boyce, V. V. Tsukruk, *ACS Appl. Mater. Interfaces* **2008**, *1*, 42.
[15] J.-H. Jang, C. Y. Koh, K. Bertoldi, M. C. Boyce, E. L. Thomas, *Nano Lett.* **2009**, *9*, 2113.
[16] S. Singamaneni, K. Bertoldi, S. Chang, J.-H. Jang, S. L. Young, E. L. Thomas, M. C. Boyce, V. V. Tsukruk, *Adv. Funct. Mater.* **2009**, *19*, 1426.
[17] K. Bertoldi, P. M. Reis, S. Willshaw, T. Mullin, *Adv. Mater.* **2010**, *22*, 361.
[18] F. Goencue, S. Willshaw, J. Shim, J. Cusack, S. Luding, T. Mullin, K. Bertoldi, *Soft Matter* **2011**, *7*, 2321.
[19] J. Li, J. Shim, J. Deng, J. T. B. Overvelde, X. Zhu, K. Bertoldi, S. Yang, *Soft Matter* **2012**, *8*, 10322.
[20] X. Zhu, G. Wu, R. Dong, C.-M. Chen, S. Yang, *Soft Matter* **2012**, *8*, 8088.
[21] J. T. B. Overvelde, S. Shan, K. Bertoldi, *Adv. Mater.* **2012**, *24*, 2337.
[22] J. Shim, C. Perdigou, E. R. Chen, K. Bertoldi, P. M. Reis, *Proc. Natl. Acad. Sci. USA* **2012**, *109*, 5978.
[23] S. Willshaw, T. Mullin, *Soft Matter* **2012**, *8*, 1747.
[24] S. H. Kang, S. Shan, W. L. Noorduin, M. Khan, J. Aizenberg, K. Bertoldi, *Adv. Mater.* **2013**, *25*, 3380.
[25] G. Wu, Y. Xia, S. Yang, *Soft Matter* **2014**, *10*, 1392.
[26] S. Shan, S. H. Kang, P. Wang, C. Qu, S. Shian, E. R. Chen, K. Bertoldi, *Adv. Funct. Mater.* **2014**, *24*, 4935.
[27] X. L. Zhu, Y. Zhang, D. Chandra, S. C. Cheng, J. M. Kikkawa, S. Yang, *Appl. Phys. Lett.* **2008**, *93*, 161911.
[28] D. Krishnan, H. T. Johnson, *J. Mech. Phys. Solids* **2009**, *57*, 1500.
[29] J. N. Grima, K. E. Evans, *J. Mater. Sci. Lett.* **2000**, *19*, 1563.
[30] J. N. Grima, R. Jackson, A. Alderson, K. E. Evans, *Adv. Mater.* **2000**, *12*, 1912.
[31] Y. Ishibashi, M. Iwata, *J. Phys. Soc. Jpn.* **2000**, *69*, 2702.
[32] A. A. Vasiliev, S. V. Dmitriev, Y. Ishibashi, T. Shigenari, *Phys. Rev. B* **2002**, *65*, 7.
[33] J. N. Grima, A. Alderson, K. E. Evans, *Comp. Methods Sci. Technol.* **2004**, *10*, 137.
[34] M. Taylor, L. Francesconi, M. Gerendas, A. Shanian, C. Carson, K. Bertoldi, *Adv. Mater.* **2014**, *26*, 2365.
[35] Y. Cho, J. H. Shin, A. Costa, T. A. Kim, V. Kunin, J. Li, S. Y. Lee, S. Yang, H. N. Han, I. S. Choi, D. J. Srolovitz, *Proc. Natl. Acad. Sci. USA* **2014**, *111*, 17390.
[36] R. Lakes, *J. Mater. Sci.* **1991**, *26*, 2287.
[37] D. Prall, R. S. Lakes, *Int. J. Mech. Sci.* **1997**, *39*, 305.
[38] A. Alderson, K. L. Alderson, D. Attard, K. E. Evans, R. Gatt, J. N. Grima, W. Miller, N. Ravirala, C. W. Smith, K. Zied, *Compos. Sci. Technol.* **2010**, *70*, 1042.
[39] K. Sun, A. Souslov, X. Mao, T. C. Lubensky, *Proc. Natl. Acad. Sci. USA* **2012**, *109*, 12369.
[40] J. N. Grima, K. E. Evans, *J. Mater. Sci.* **2006**, *41*, 3193.
[41] H. Mitschke, G. E. Schröder-Turk, K. Mecke, P. W. Fowler, S. D. Guest, *Europhys. Lett.* **2013**, *102*, 66005.
[42] C. L. Kane, T. C. Lubensky, *Nat. Phys.* **2014**, *10*, 39.
[43] S. Hyun, S. Torquato, *J. Mater. Res.* **2002**, *17*, 137.
[44] R. G. Hutchinson, N. A. Fleck, *ZAMM* **2005**, *85*, 607.
[45] A. V. Dyogtyev, I. A. Sukhoivanov, R. M. De La Rue, *J. Appl. Phys.* **2010**, *107*, 013108.
[46] D. Jang, L. R. Meza, F. Greer, J. R. Greer, *Nat. Mater.* **2013**, *12*, 893.
[47] P. Russell, *Science* **2003**, *299*, 358.
[48] K. Tantikom, Y. Suwa, T. Aizawa, *Mater. Trans.* **2004**, *45*, 509.
[49] J. N. Grima, A. Alderson, K. E. Evans, *Phys. Status Solidi B* **2005**, *242*, 561.